Comparison of Synthetic Aperture Radar Autofocus Techniques — Phase Gradient vs Subaperture*

Terry M. Calloway† Charles V. Jakowatz, Jr. Paul A. Thompson Paul H. Eichel

Sandia National Laboratories
Albuquerque, New Mexico 87185-5800

ABSTRACT

Two methods of focusing synthetic aperture radar (SAR) images are compared. Both a conventional subaperture cross-correlation method and a new phase gradient autofocus (PGA) algorithm developed at Sandia National Laboratories are shown to perform well if high-order phase errors are not present. With the introduction of significant high-order phase errors [*e.g.*, due to uncompensated platform motion], both algorithms suffer a loss in performance. However, relative performance degradation is less for PGA than for the subaperture focusing technique. An explanation is presented for the observed behavior of the two autofocus techniques.

1 INTRODUCTION

Two methods of focusing a synthetic-aperture radar (SAR) image are compared in this article: subaperture cross-correlation and phase gradient autofocus (PGA). A **focused image** may be defined as one from which the impulse response, or *point spread function* (PSF), has been deconvolved. After this has been accomplished, a point target will appear in an image only at a single picture element (pixel).

Assume that the PSF depends upon cross-range only. The Fourier transform of the PSF along the cross-range direction is its range-compressed phase history — a function of aperture only. The range-compressed phase history of a PSF is complex-valued with magnitude and phase that vary along the aperture. In this paper the phase of the point spread function's Fourier transform is referred to as the *phase error function* or, simply, the *phase function* associated with the PSF.

A nonlinear phase error function influences image focus and contrast. Figure 1 shows four phase error functions and their corresponding point spread functions.

Figure 1a is the phase function of the ideal PSF shown in Figure 1b. Figure 1c is the phase function of the low-resolution PSF shown in Figure 1d. A low-order phase function produces a wide main lobe — the chief characteristic of a poorly-focused image.

As shown in Figures 1e and 1f, a high-order phase function degrades image contrast. Qualitatively, contrast is the ratio of main lobe magnitude to side lobe magnitude. Although the main lobe of Figure 1f is narrow, indicating satisfactory focus; the side lobes are large, indicating poor contrast. If high-order phase errors are present, they reduce the observed signal-to-clutter ratio of an image — limiting the useful range of the SAR system.

*This work was supported by the U. S. Department of Energy under contract DE-AC04-76DP00789
†To whom requests for reprints should be addressed, at Sandia National Laboratories, Division 9117, Albuquerque, NM 87185-5800.

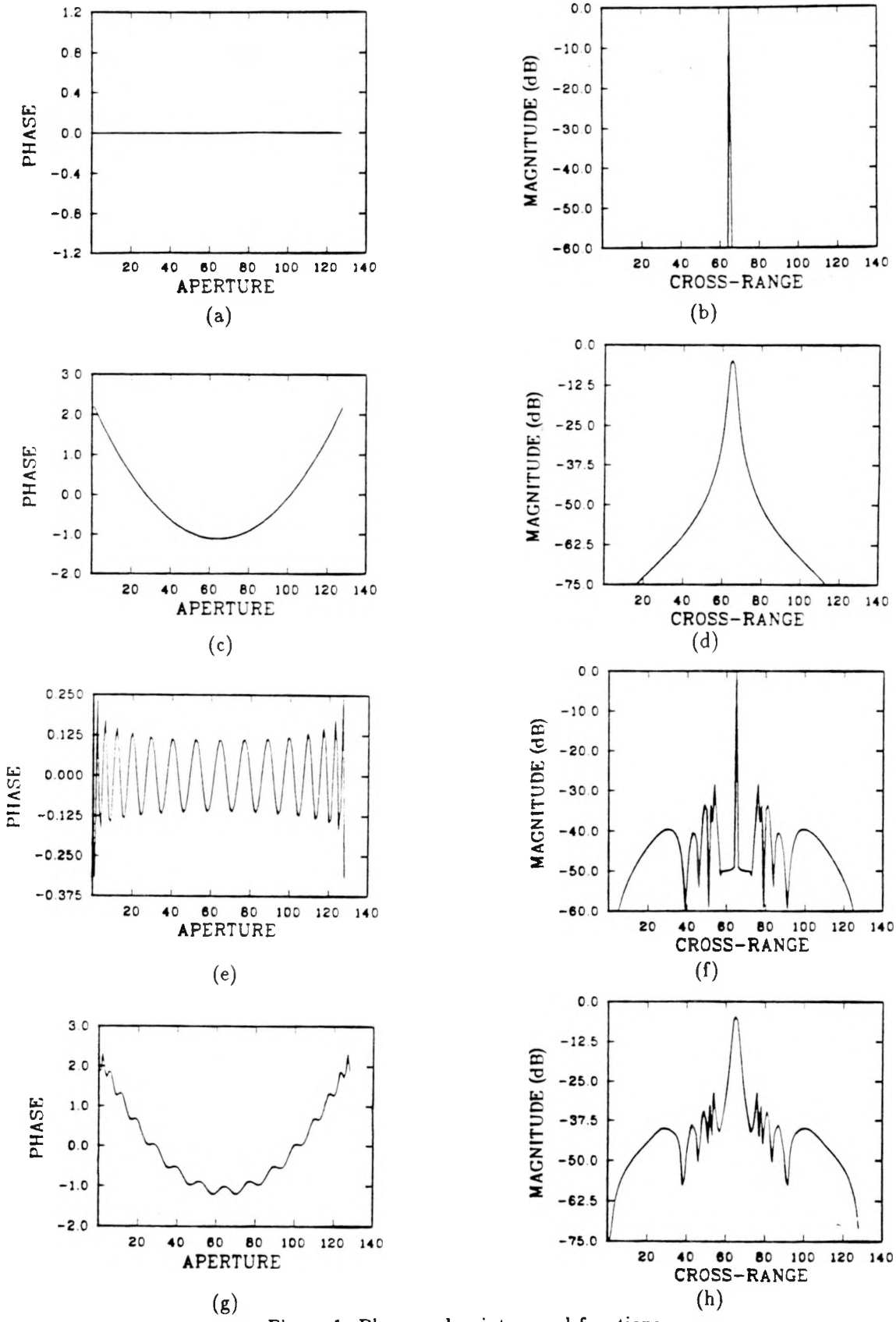

Figure 1: Phase and point spread functions

A linear combination of low-order and high-order phase errors is illustrated in Figure 1g. Both poor resolution and poor contrast are evident in the corresponding PSF shown in Figure 1h.

The subaperture technique analyzed here has been called *map drift*.[1] If a second-degree phase function exists along the full aperture, then a pair of images (maps) formed from two different subapertures will appear translated with respect to one another. That is, a second-order phase function will cause the subaperture maps to drift apart. The *map drift* is the relative separation between map pairs. Cross-correlation of each pair of maps yields estimates of the map drifts which are related to the phase function that must be removed in order to focus the image.

If contrast is poor, as in Figure 1f, then the error variance of a map drift estimate will be correspondingly large. To minimize variance of a drift estimate, one should maximize contrast before cross-correlating the maps. From the preceding remarks one concludes that: (1) high-order phase errors are associated with poor contrast, (2) poor contrast increases the error in the map drift estimate, (3) increasing the error in the drift estimate degrades focusing performance. Consequently, one should remove as much of the higher-order phase errors as possible before cross-correlating to remove lower-order phase errors.

The phase gradient algorithm (PGA) developed at Sandia National Laboratories uses a wide cross-range window to remove high-order phase errors during early iterations, then removes residual lower-order phase errors during subsequent iterations by decreasing the window width.[2] This is contrary to Brown and Ghiglia's[1] earlier speculation that, "As higher-order terms are calculated, the region of support could be appropriately enlarged."

It has been shown that the phase gradient function computed by PGA is an unbiased, minimum-variance linear estimate.[3] Experience with the algorithm indicates that it converges to a well-focused image under a wide variety of conditions, including low signal-to-clutter ratio and uncompensated platform motion.

The phase error function as computed by either method is valid only if the true phase function does not vary too abruptly along the aperture. The sampling rate along the aperture must be high enough to record the most abrupt changes present in the phase function.

Both the map drift and the phase gradient autofocus algorithms work satisfactorily even if there is not an isolated, strong, point-scatterer in the image. Both algorithms perform as intended if no significant high-order phase errors exist. However, if high-order phase errors are present, PGA outperforms map drift.

2 OBSERVED FOCUSING PERFORMANCE

Both simulated data and field test data are used in this analysis. The simulated data consists of an ideal point-target in the center of a scene with clutter noise added to each channel of the quadrature demodulated data. The field test data consists of a well-focused radar image to which phase errors are added.

Referring to the aperture domain, peak signal strength is denoted as a_s and standard deviation of the additive clutter noise as σ per channel. Figure 2 shows the average phase error variance for 100 trials of map drift and 100 trials of PGA. Figures 2a–d correspond to a_s^2/σ^2 ratios of 40dB, 50dB, 60dB, and 70dB, respectively.

In addition to the parametric sensitivity analysis of phase error variance under controlled conditions of known signal-to-clutter ratio (SCR) and known phase error, a test was performed on a well-focused SAR image of unknown SCR. A 16^{th}-order phase error was added to blur the image, then PGA and map drift were each used to focus the blurred image.

Figure 3 shows the phase error that was applied to blur the image. Figures 4 and 5 are each one row extracted from the images that were focused with with map drift and with PGA, respectively. Figures 6 and 7 are the phase error functions estimated by map drift and by PGA, respectively. The solid curve is the true phase error and the dashed curve is the estimated phase error.

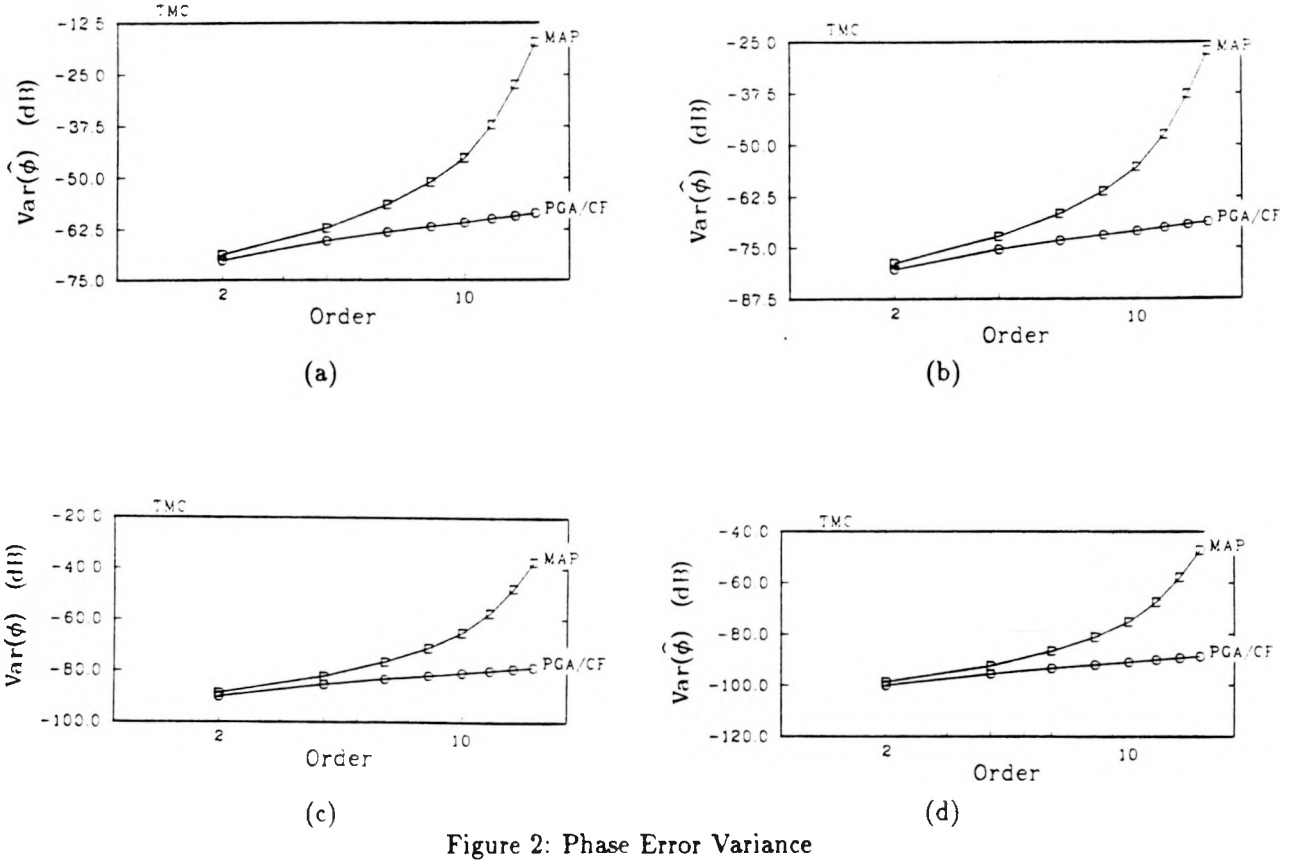

Figure 2: Phase Error Variance

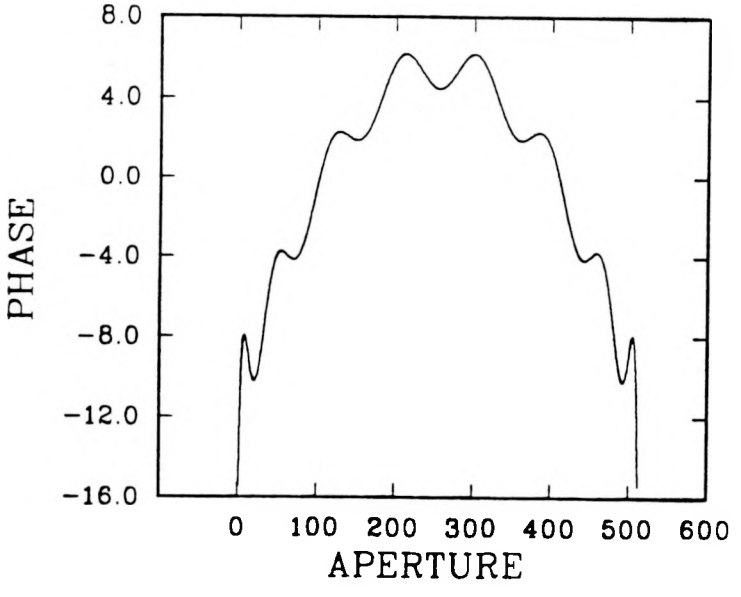

Figure 3: Sixteenth-order phase error

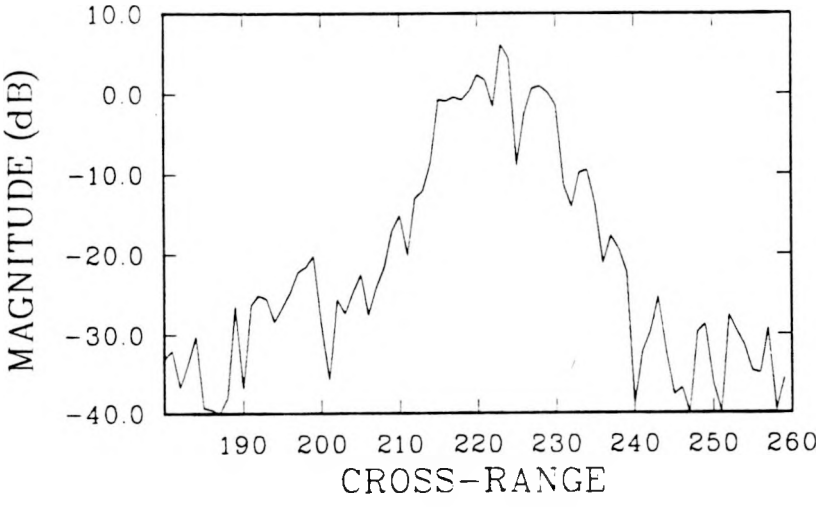

Figure 4: One row of image after map drift

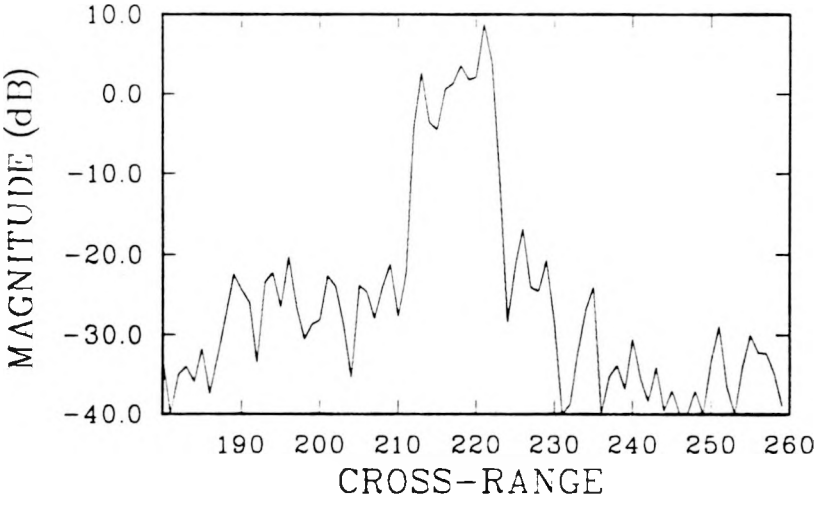

Figure 5: One row of image after PGA

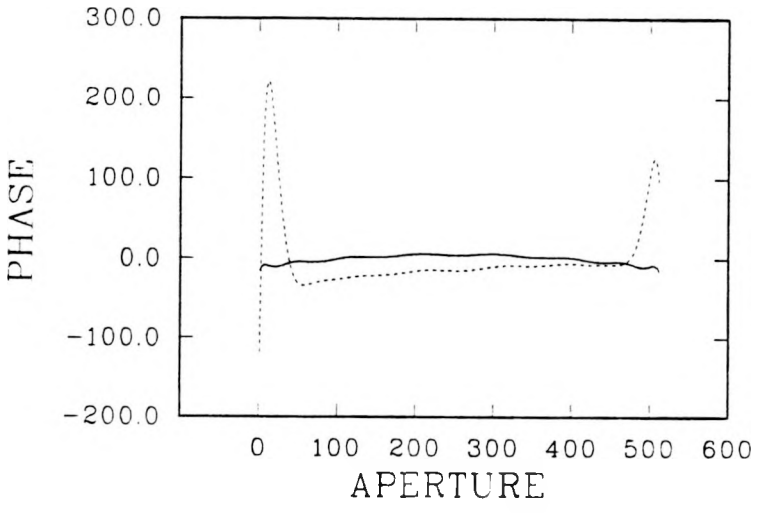

Figure 6: Phase estimated by map drift

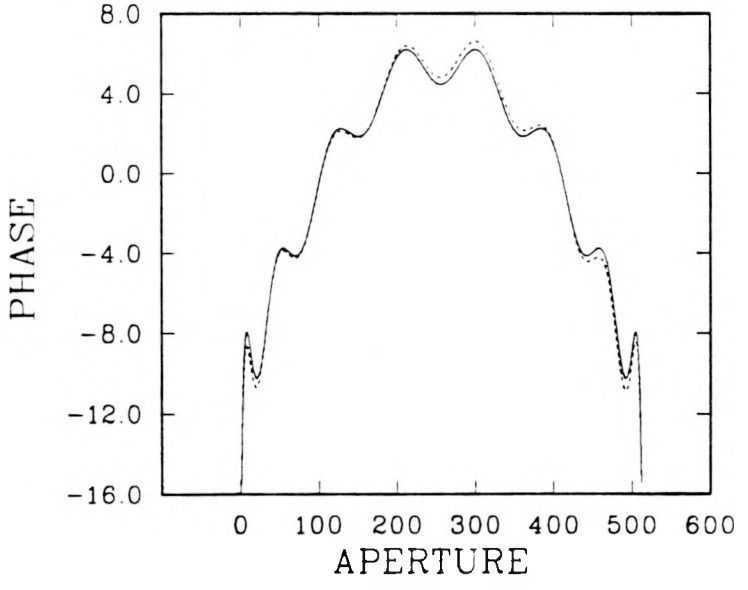

Figure 7: Phase estimated by PGA

Clearly, map drift did not provide a satisfactory estimate of the phase error. The mean squared errors for the phase error estimates of PGA and map drift are 0.097 and 2400 — a disparity of 44dB. This agrees with the results of the simulation studies that employed 16^{th}-order estimates.

Notice how the phase estimated by map drift is much worse near the edges of the aperture. Brown and Ghiglia[1] mention that "second-derivative samples are not available at the extreme endpoints of the full aperture, and therefore some extrapolation is necessary, which usually leads to errors". Perhaps some *ad hoc* technique could be developed to remedy this problem associated with map drift autofocus, which is a parametric estimation algorithm. However, with PGA (a nonparametric algorithm) the problem does not occur.

3 EXPLANATION

Next, we will present an explanation for the observed behaviors of the two autofocus techniques. The formulas obtained for drift variance and phase error variance agree with the simulation results.

3.1 SUBAPERTURE CROSS-CORRELATION

A new map drift model is presented based on piecewise linear regression instead of piecewise cubic spline regression. The spline method estimates the second derivative of the phase error function and assumes that it corresponds to the midpoint between the subapertures.[1] However, the midpoint position assignment is incorrect for higher-order phase errors, resulting in an erroneous spline-function estimate.

The new model regresses a linear phase ramp through each subaperture. No assumptions are made regarding second derivatives or their locations. Coefficients of the full-aperture phase error polynomial that best fits the observed map drifts are computed in a consistent manner even in the presence of higher-order terms. This ensures that the map drift autofocus implementation used here performs to its full potential.

The map drift (MD) algorithm estimates PSF phase along the aperture by partitioning the aperture into subapertures, forming subimages (*maps*), and cross-correlating the maps. The amount of azimuth translation, or *drift*, between maps is related to the full-aperture phase function.

Partition the full aperture T into M subapertures. The range-compressed phase history $g_i(t)$ of the i^{th} subaperture is

$$g_i(t) \equiv g(t + t_i) \operatorname{rct}\left(\frac{Mt}{T}\right)$$

where

$$t_i \equiv \frac{T}{2}\left(\frac{2i-1}{M} - 1\right) \qquad i \in \{1, 2, \ldots, M\}$$

and

$$\operatorname{rct} x \equiv \begin{cases} 1 & \text{if } |x| < 1/2 \\ 1/2 & \text{if } |x| = 1/2 \\ 0 & \text{if } 1/2 < |x| \end{cases}$$

Maps are images formed from phase-history data. For a quadratic phase error function the drift between a pair of subaperture maps provides the quadratic coefficient required to focus the full-aperture map. In this section a mathematical expression that relates the phase error computed by map drift autofocus to the estimated map drifts is derived.

Assume that each subaperture phase history $g_i(t)$ is modeled as

$$\begin{aligned} g_i(t) &= s_i(t) + n_i(t) \\ &= a_{si}e^{j\phi_{si}(t)} + a_{ni}(t)e^{j\phi_{ni}(t)} \end{aligned} \tag{1}$$

The variance σ_{ni}^2 of the complex noise n_i is

$$\sigma_{ni}^2 = 2\sigma^2$$

where each of the real and imaginary components of n_i has variance σ^2. The Fourier transform $G(\omega)$ of $g(t)$ is one range bin of a SAR complex-valued image.

$$G(\omega) \equiv \mathcal{F}\{g(t)\}$$

For a point target Equation 1 is

$$\begin{aligned} g &= a_s e^{j\phi_s} + a_n e^{j\phi_n} \\ &= a_s a_m e^{j(\phi_s+\phi_m)} \end{aligned}$$

If $\sigma \ll a_s$, then

$$g \approx a_s\, e^{j(\phi_s+\phi_m)}$$

If the clutter-to-noise ratio is small enough, the observed amplitude is approximately equal to the amplitude of the uncluttered signal. However, a small phase error ϕ_m is added to the signal phase.[4,p.43]

If the correct phase function were estimated and applied, the focused result would be

$$g_{foc} = a_s e^{j\phi_m}$$

Consequently, even if the phase error were estimated correctly and removed entirely, there would still be a residual phase modulation ϕ_m due to clutter.

The signal phase ϕ_{si} along the i^{th} subaperture is

$$\phi_{si}(t) \equiv \phi_s(t + t_i) \qquad\qquad |t| < \frac{T}{2M}$$

Assume that $\phi_{\ell i}(t)$ is the best linear estimator of the i^{th} subaperture phase $\phi_{si}(t)$. Specifically, assume that $\phi_{\ell i}(t)$ is the linear function that fits $\phi_{si}(t)$ with minimum mean square error on the interval $[-\frac{T}{2M}, \frac{T}{2M}]$. Let the Taylor series coefficients b_{0i} and b_{1i} of

$$\phi_{\ell i}(t) \equiv b_{0i} + b_{1i}t \tag{2}$$

be defined such that

$$\mathcal{E}_i^2 \equiv \left\langle \|\phi_{si} - \phi_{\ell i}\|^2 \right\rangle \tag{3}$$

is minimized. The solution is

$$\begin{aligned} b_{1i} &= \frac{\langle (t-\bar{t})\ [\phi_{si} - \bar{\phi}_{si}] \rangle_M}{\langle (t-\bar{t})^2 \rangle_M} \\ b_{0i} &= \bar{\phi}_{si} - b_{1i}\langle t \rangle_M \\ &= \bar{\phi}_{si} \end{aligned} \tag{4}$$

where

$$\bar{\phi}_{si} \equiv \langle \phi_{si} \rangle_M$$

and the mean value operator $\langle \bullet \rangle_M$ is defined as

$$\langle \phi \rangle_M \equiv \frac{M}{T} \int_{-T/2M}^{T/2M} \phi \, dt$$

If each residual subaperture error $\mathcal{E}_i^2$ is negligible, then each subaperture map is a translated version of the image formed from the full aperture.

$$\begin{aligned} I_i(\omega) &\equiv \mathcal{F}\{g_i(t)\} \\ &= \mathcal{F}\left\{a_s e^{j(\phi_s + b_{1i}t)}\right\} \\ &\approx I(\omega + b_{1i}) \end{aligned}$$

A reduction in aperture size is necessary to estimate high-order phase errors; however, utilizing only part of the available aperture data causes a corresponding decrease in cross-range resolution.[5,p.303] The inevitable trade-off between aperture size and cross-range resolution explains why map drift autofocus does not perform as well as phase gradient autofocus in the face of high-order phase errors.

If the phase function $\phi_{si}(t)$ is of order N, then expand $\phi_s(t)$ in an N^{th}-degree Taylor series. [There should be no confusion between the noise magnitude a_n and the coefficients a_k of the Taylor series.]

$$\phi_s(t) = \sum_{k=0}^{N} a_k t^k \qquad |t| < \frac{T}{2} \tag{5}$$

Substituting Equation 5 into Equation 4, the linear coefficient b_{1i} is evaluated as

$$\begin{aligned} b_{1i} = \frac{3}{2}\left(\frac{2M}{T}\right)^3 \sum_{p=2}^{N} \Bigg\{ & \frac{1}{p+2}\left[\left(t_i + \frac{T}{2M}\right)^{p+2} - \left(t_i - \frac{T}{2M}\right)^{p+2}\right] \\ & - \frac{t_i}{p+1}\left[\left(t_i + \frac{T}{2M}\right)^{p+1} - \left(t_i - \frac{T}{2M}\right)^{p+1}\right] \Bigg\} a_p \end{aligned}$$

This expression predicts the drift between the i^{th} subaperture map and the full-aperture map. However, the conventional map drift algorithm measures drifts between pairs of subaperture maps. Because residual phase error $\mathcal{E}^2$ for the full-aperture map (unfocused image) could be significant, cross correlation of a subaperture map with a full-aperture map may yield unreliable estimates of b_{1i}.

Denote the drift between maps i and j as ω_{ij}.

$$\omega_{ij} = b_{1j} - b_{1i} \tag{6}$$

If the number M of subapertures equals the degree N of the polynomial phase estimate $\widehat{\phi}_s(t)$, then it is possible to compute $(N-1)N/2$ drifts Ω_m between the maps formed from all combinations of non-overlapping subapertures.

$$\begin{aligned} \Omega_m &= \omega_{ij} \\ m &= \frac{1}{2}(i-1)(2N-i) + j - i\,, \qquad 1 \le i < j \le N \\ &= \frac{1}{2}(i+1)(2N-i) + j - N \end{aligned}$$

Equation 6 defines $(N-1)N/2$ linear equations in the $N-1$ unknown Taylor coefficients $\{a_2, a_3, \ldots, a_N\}$. A concise matrix representation is

$$\Omega = \mathbf{B}\mathbf{a} \tag{7}$$

The least-squares solution $\hat{\mathbf{a}}$ of this system is

$$\begin{aligned} \hat{\mathbf{a}} &= \left(\mathbf{B}^T\mathbf{B}\right)^{-1}\mathbf{B}^T\Omega \\ &= \mathbf{B}^{\#}\Omega \end{aligned} \tag{8}$$

The resulting estimate $\widehat{\phi}_2$ of the phase error function is

$$\widehat{\phi}_2(t) = \sum_{p=2}^{N} a_p t^p$$

Hahn[6] has analyzed the variance of cross-correlator time delays in regard to passive sonar bearing estimation. By properly filtering each channel of data, the mean squared error of all the delay estimates can achieve the Cramér-Rao lower bound.

For the simulated data, the map drift variance achieves the Cramér-Rao lower bound. Unfortunately, the lower bound for subaperture cross-correlation increases as M^3, where M is the number of subapertures.

Denote the noise variance per channel as σ^2, the peak signal intensity as a_s, the full-aperture length as T, the model order as M, the number of aperture samples as L, and the number of range cells as K. Let the aperture variable be represented as t and let its Fourier transform domain variable (cross-range) be designated as f. The Cramér-Rao lower bound σ_f^2 for each map drift estimate $\widehat{f}_{ij}$ between maps i and j is[6,7,8]

$$\begin{aligned} \mathrm{Var}\left(f_{ij}\right) &\geq \sigma_f^2 \\ &= \left(\frac{3}{4\pi^2 LK}\right)\left(\frac{2\sigma^2}{a_s^2}\right)\left(\frac{2M}{T}\right)^3 \end{aligned} \tag{9}$$

In the computer simulations $L = 1024$ and it is assumed that $T = 2$ and $K = 1$. Equation 9 then simplifies to

$$\mathrm{Var}\left(f_{ij}\right) \geq \left(\frac{3}{4096\pi^2}\right)\left(\frac{\sigma}{a_s}\right)^2 M^3$$

Equation 9, a result of estimation theory, quantifies the qualitative observation of Brown and Ghiglia[1] that "the accuracy of the cross correlation of two adjacent maps implicit in the map-drift measurement decreases with decreasing subaperture length".

Figure 8 shows the map drift variances that produced the phase error variances illustrated in Figure 2. The dashed lines are lower bounds as given by Equation 9. For the controlled conditions existing in the computer simulations, the map drift estimates achieve their Cramér-Rao bounds. In a mean square sense, no better unbiased estimates can be found.

3.2 FULL-APERTURE PHASE GRADIENT

To compare PGA (a nonparametric autofocus algorithm) with map drift (a parametric autofocus algorithm) a polynomial is regressed onto the PGA phase error estimate. Projecting the PGA estimate onto a set of orthonormal polynomials (specifically, Legendre polynomials Y_p) gives

$$\widehat{\phi}_{PGA/CF}(t) = \sum_{p=2}^{M} v_p Y_p(t)$$

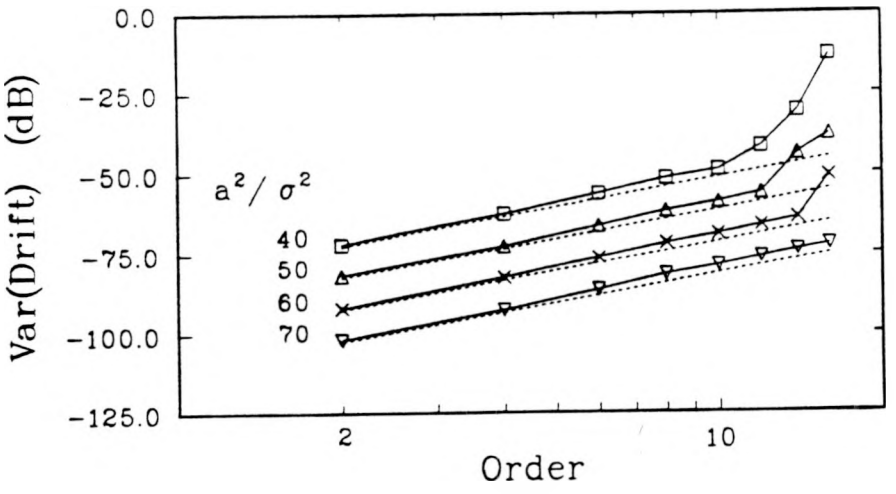

Figure 8: Drift Variance

with a variance of

$$\begin{aligned} \mathrm{Var}\left(\widehat{\phi}_{PGA/CF}\right) &= \sum_{p=2}^{M} v_p^2 \\ &= \frac{M-1}{KL}\left(\frac{\sigma}{a_s}\right)^2 \end{aligned}$$

Here M is model order, K is the number of range bins, L is the number of aperture samples, a_s is the peak signal strength in the aperture domain, and σ is the noise standard deviation per channel. This linear dependence on model order M agrees with the results shown in Figure 2.

4 RESULTS

The proposed explanation for map drift's performance in the face of high-order phase errors agrees with the results of focusing simulated SAR images. For a wide range of signal-to-clutter ratios, the phase error variance of PGA can be 40dB smaller than that of map drift.

To confirm further the simulation results, we applied a known phase error to a well-focussed SAR image obtained during a field test of a radar system built at Sandia National Laboratories. An absolute variance prediction is more difficult to make for an actual SAR image, because the signal-to-clutter ratio (SCR) and the phase error are unknown. However, the mean squared error (MSE) of the phase function estimated by PGA with a 16^{th}-order curve fit is approximately 40dB smaller than the MSE of the phase function estimated by map drift. This performance improvement corrobrates results of the parametric sensitivity analysis, which employed simulated SAR images with known SCR and phase error.

5 CONCLUSIONS

Either phase gradient autofocus (PGA) or cross-correlation of subapertures can be used effectively to focus a synthetic aperture radar image if no high-order phase errors are present. If high-order phase errors exist (due, for example, to uncompensated platform motion, to clock drift in the local oscillator, or to random delays in the propagation path), then both PGA and map drift suffer a loss in performance. However, the phase error variance of map drift increases more rapidly than does that of PGA as higher-order phase errors are estimated.

6 ACKNOWLEDGEMENT

We thank our colleagues D. C. Ghiglia for explaining the conventional subaperture autofocus algorithm, and D. E. Wahl for identifying a problem with a peak-search algorithm. M. J. Hicks, who provided block diagrams and MATLAB^{TM} source code for a subaperture autofocus algorithm, also deserves recognition. D. M. Shead developed fast-executing FORTRAN code for the parametric sensitivity analysis.

REFERENCES

1. W. D. Brown and D. C. Ghiglia, "Some methods for reducing propagation-induced phase errors in coherent imaging systems — I. formalism," *Journal of the Optical Society of America*, vol. 5, pp. 924–941, June 1988.

2. P. H. Eichel, D. C. Ghiglia, and C. V. Jakowatz, Jr., "Speckle processing method for synthetic-aperture radar phase correction," *Optics Letters*, vol. 14, pp. 1–3, January 1989.

3. P. H. Eichel and C. V. Jakowatz, Jr., "Phase-gradient alogorithm as an optimal estimator of the phase derivative," *Optics Letters*, vol. 14, pp. 1101–1103, October 1989.

4. A. W. Rihaczek, *Principles of High-Resolution Radar*. Los Altos, CA: Peninsula Publishing, 1985.

5. L. H. Koopmans, *The Spectral Analysis of Time Series*. Vol. 22 of *Probability and Mathematical Statistics*, New York, NY: Academic Press, 1974.

6. W. R. Hahn, "Optimum signal processing for passive sonar range and bearing estimation," *Journal of the Acoustical Society of America*, vol. 58, pp. 201–207, July 1975.

7. T. M. Calloway, *Comparison of Autofocus Methods for Synthetic Aperture Radar*. PhD thesis, University of New Mexico, Albuquerque, NM, to be published. Department of Electrical and Computer Engineering.

8. A. H. Quazi, "An overview on the time delay estimate in active and passive systems for target localization," *IEEE Transactions on Acoustics, Speech, and Signal Processing*, vol. ASSP-29, pp. 527–533, June 1981.